Journal of Ornithology (2023) 164:591–603
https://doi.org/10.1007/s10336-022-02042-8

ORIGINAL ARTICLE

The uropygial gland of the Great Cormorant (*Phalacrocorax carbo*): I. Morphology

Nadine Stangier[1] · Sandra Sandhöfer[1,2] · Axel Mosig[2] · Claudia Distler[1]

Received: 12 September 2022 / Accepted: 21 December 2022 / Published online: 11 January 2023

Abstract

To further our knowledge of the basis of the wing-spreading behavior of cormorants, we compared the feathers of cormorants with a diving and a dabbling duck. Only the cormorant shows the division into a closed vane next to the rhachis and an open vane in the periphery of the feather. Macroscopically, the uropygial gland of the Great Cormorant (*Phalacrocorax carbo*) is bilobed, the papilla wears circlet feathers of type I. Histologically, the uropygial gland of the cormorant consists of tightly packed glandular tubules separated by internal septa. These tubules can be divided into three zones based on their laminar appearance. They transition into secretion-filled ducts that lead to the papilla. There is no central storage chamber. By contrast, the uropygial gland of the rock pigeon (*Columba livia*) contains a large central storage chamber, the glandular tissue is limited to the periphery of the gland. Thus, the histological organization of the cormorant uropygial gland is similar to many other aquatic birds. To elucidate the complex internal structure, we additionally reconstructed the uropygial gland three-dimensionally.

Keywords Cormorant · *Aythya fuligula* · *Mareca penelope* · Feather structure · Uropygial gland · 3D reconstruction

Zusammenfassung

Die Bürzeldrüse des Kormorans (*Phalacrocorax carbo*). I. Morphologie

Um die Ursachen des charakteristischen Flügelspreizverhaltens des Kormorans aufzuklären, wurde zunächst die Federstruktur des Kormorans mit der Federstruktur einer Tauchente (*Aythya fuligula*) und einer Schwimmente (*Mareca penelope*) verglichen. Nur die Deckfedern des Kormorans zeigen eine Unterteilung in eine geschlossene Fahne nahe der Rhachis und eine offene Fahne in der Peripherie der Feder. Makroskopisch ist die Bürzeldrüse des Kormorans zweilappig, die Papille trägt einen Bürzeldocht aus modifizierten Daunenfedern (Typ I). Die Bürzeldrüse besteht aus dicht gepackten Drüsenschläuchen und ist durch innere Septen unterteilt. Aufgrund ihrer Schichtung können die Drüsenschläuche in drei Zonen unterteilt werden. Sie gehen in mit Sekret gefüllte Gänge über, die zur Papille ziehen. Eine zentrale Speicherkammer fehlt. Bei der Felsentaube (*Columba livia*) dagegen enthält die Bürzeldrüse eine sehr große Speicherkammer und das Drüsenepithel ist auf die Peripherie der Drüse beschränkt. Die histologische Struktur der Bürzeldrüse des Kormorans ähnelt also der vieler anderer Wasservögel. Erstmalig wurde die innere Struktur der Bürzeldrüse von Kormoran und Felsentaube auch drei-dimensional rekonstruiert.

Introduction

The Great Cormorant (*Phalacrocorax carbo*) is one of only few water birds that have to "dry" their feathers after diving. Thus, these birds are not only known for their diving abilities up to a depth of about 35 m coupled with a great prey capture efficiency (Quintana et al. 2007), but also for their wing-spreading behavior thereby exposing their feathers to the sun and the wind. This behavior has been linked, among

Communicated by I. Moore.

✉ Claudia Distler
distler@neurobiologie.rub.de

[1] General Zoology & Neurobiology, Ruhr-University Bochum, Bochum, Germany

[2] Bioinformatics Group, Faculty of Biology and Biotechnology, Ruhr-University Bochum, Bochum, Germany

others, to the partial wettability of the cormorant's feathers (Johnsgard 1993; Schmid et al. 1995; Rijke and Jesser 2011). This wettability reduces the air cushion surrounding the skin and thus buoyancy (Schmid et al. 1995; Sellers 1995), but also increases energy demand especially in cool water due to heat loss (Gremillet et al. 2001).

Several anatomical and modeling studies have clearly linked this wettability to the unusual structure of the cormorant's feathers (Rijke 1968; Gremillet et al. 2005; Rijke and Jesser 2011; Srinivasan et al. 2014). The densely spaced barbules together with a low spacing ratio of the barbules in combination with the hydrophobic properties of preen oil are supposedly responsible for spontaneous dewetting of the feathers after a dive. The wing-spreading seems to facilitate the spontaneous drying if pinning sites are present (Srinivasan et al. 2014). Nevertheless, an additional role of the uropygial secretion, i.e., preen oil has not been ruled out.

The uropygial gland is the most conspicuous gland in the avian skin. Its secretion is spread on the feathers during preening. Besides aiding in waterproofing the plumage, the uropygial secretion supposedly improves feather integrity (Elder 1954; Giraudeau et al. 2010), makes feather color appear brighter (e.g., Moreno-Rueda 2017), and has antibacterial, antifungal and antiparasitic properties (Jakob and Ziswiler 1982; Bandyopadhyay and Bhattacharyya 1999; Shawkey et al. 2003) thus influencing the microorganism community of the plumage (e.g., Møller et al. 2010). In this context, the coloring of hoopoe eggs with uropygial secretion may protect the embryo against pathogenic bacteria (Soler et al. 2014). In addition, the uropygial secretion is a source of body odor and thus potentially involved in intraspecific communication, i.e., in sex and kin recognition, mate choice, and health status and aggression signaling (e.g., Jakob et al. 1979; Amo et al. 2012; Reynolds et al. 2017; Whittaker et al. 2018; Caspers et al. 2022 and references therein) as well as in nest crypsis (e.g., Reneerkens et al. 2005; Soini et al. 2007).

By contrast, beyond a general description of related species (Jakob and Ziswiler 1982; Johnston 1988) the morphology of the uropygial gland of the Great Cormorant and the composition of its preen oil have not been investigated in detail. Thus, in the present study we for the first time present a histological analysis of the cormorant uropygial gland. The biochemical composition of the Great Cormorant's uropygial secretion is presented in the accompanying paper (Holste et al. submitted).

Material and methods

Animals

Altogether five cormorants (*Phalacrocorax carbo*) were used for the present investigation, two for the histological analysis of the uropygial gland, and three for the biochemical analysis of the uropygial secretion (see accompanying paper, Holste et al. submitted). The birds were shot as lethal control measure and their uropygial glands were analyzed (permit 67.1–2.03.20-pi, 09–2014), Untere Naturschutzbehörde Rhein-Sieg-Kreis, and permit 35/61.92.16 (001/16), Untere Landschaftsbehörde Hochsauerlandkreis) during winter 2015/2016. For comparison, the uropygial glands of two adult homing pigeons (*Columba livia*) and of one domesticated Muscovy Duck (*Cairina moschata*) were analyzed. Both the pigeons and the Muscovy Duck were obtained from local breeders.

Histology

After dissection, the uropygial glands were measured, weighed, and the relative gland mass (RGM) was calculated as gland mass / body mass × 100. After removal of the gland, the tissue was fixed in Bouin solution and embedded in paraffin. Serial 10 µm thick sections were cut at a microtome (Leica RM 2145) in the horizontal (one gland), coronal (left hemisphere of the second gland), or parasagittal plane (right hemisphere of the second gland), and stained using a combination of Goldner's trichrome technique (Goldner 1938) with Gomori's aldehyde-fuchsin-Goldner (AFG) method (Gomori 1950).

Analysis

The feathers of a cormorant, a Tufted Duck (*Aythya fuligula*) and a Eurasian Widgeon (*Mareca penelope*) were photographed with a Nikon D70 camera equipped with a 60 mm lens and at a microscope (Zeiss AxioZoom V16). Image stacks were compiled with ZEN blue 2.3 software. Histological sections were photographed at a Zeiss Stemi 2000 binocular and a photomicroscope (Zeiss Axioplan) using a Canon eOS 600D camera. Brightness and contrast of the photographs were adjusted in Adobe Photoshop 5.0.

For the 3D-reconstruction, the sagittal sections of the cormorant and the pigeon uropygial gland were scanned at a confocal microscope (Leica TCS SP5 II equipped with a DPSS 561 laser) at an intersection distance of 200 µm. The images were converted to tiff-files using ImageJ. Then the sections were redrawn in Coreldraw X6 and the various structures as connective tissue, excretory tubules, cavities, and fat tissue were coded in different colors for subsequent

reconstruction. For 3D reconstructions, the images were spatially aligned and adjusted to a unique size for subsequent stacking to a 3D image. Subsequently, the image stacks of pigeon uropygial gland underwent intensity thresholding followed by morphological opening and closing operations, so that cavities could be identified and visualized distinctly. For 3D reconstruction of cavities in cormorant uropygial gland, cavities needed to be annotated manually using CorelDraw before registration, size adjustment and stacking. Size adjustment and registration was performed using FiJI (Schindelin et al. 2021), while thresholding and morphological filtering were implemented as in-house MATLAB scripts. 3D visualizations were produced using Vaa3D (Peng et al. 2010).

Results

Feather morphology

The morphology of cormorant feathers has been described before (Gremillet et al. 2005; Srinivasan et al. 2014). Nevertheless, we demonstrate it here in comparison with three other water birds, the diving Tufted Duck and a dabbling duck, the Eurasian Widgeon as well as a Muscovy Duck. Figure 1A shows a typical feather from the ventral rump of a Great Cormorant. It is also representative for feathers from the breast and the back of the animal. The cormorant feather is characterized by a closed vane close to the rhachis surrounded by a loose distal part where the barbs are not connected by barbules (Fig. 1B, C). By contrast, the feathers of the Tufted Duck (Fig. 2) and the European Widgeon (Fig. 3) have an appearance also typical for terrestrial birds, with the proximal parts of the feather characterized by down-like barbs not conjoined by barbules. Only the distal parts of the feather bear a closed vane built by interconnected barbules over the whole extent of the barbs. Thus, the foraging behavior of these birds is not directly correlated with feather morphology: cormorant and Tufted Ducks both dive to the bottom of the water body whereas the European Widgeon does not dive. Only the cormorant shows the typical wing spreading behavior. The structure of the wing feathers of the cormorant does not differ from that of other aquatic birds (e.g., the European Widgeon and the Muscovy Duck) (supplementary Fig. S1). Apart from the most proximal part of the feather, the barbs are interconnected by barbules over

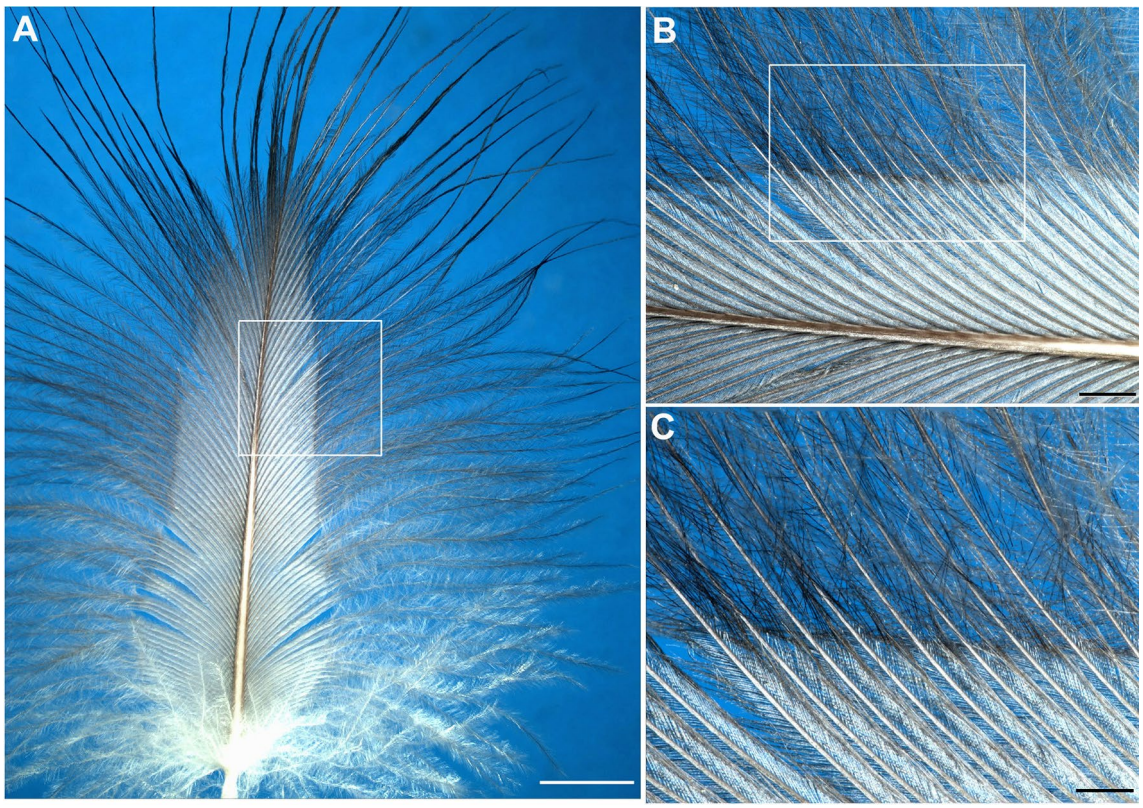

Fig. 1 Photograph of a feather from the ventral rump of a Great Cormorant (*Phalacrocorax carbo*) demonstrating the morphology typical also for feathers from the breast and the back. **A**: overview, **B**, **C**: details of the transition zone of the closed and the open vane. Inset in **A** shows the location of the detail seen in **B**, inset in **B** shows location of detail depicted in **C**. Scale bars represent 5 mm (**A**), 1 mm (**B**), and 0.5 mm (**C**)

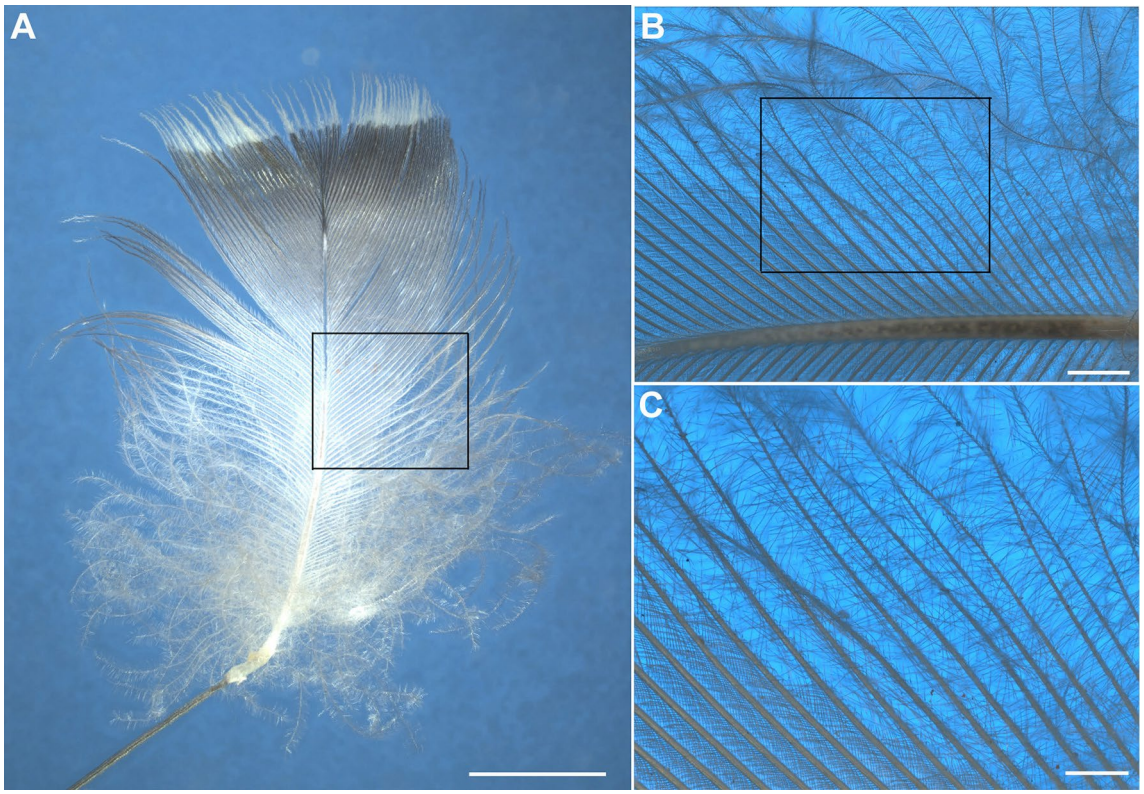

Fig. 2 Photograph of a feather from the ventral rump of a Tufted Duck (*Aythya fuligula*) demonstrating the morphology typical also for feathers from the breast and the back. **A**: overview, **B**, **C**: details of the transition zone of the closed and the open vane. Inset in A shows the location of the detail seen in B, inset in B shows location of detail depicted in **C**. Scale bars represent 5 mm (**A**), 1 mm (**B**), and 0.5 mm (**C**)

the whole extent of the feather thus forming a complete airfoil essential for flight.

Dissection of the uropygial gland

As in other birds, the uropygial gland of the cormorant is located subcutaneously dorsal of the caudal vertebrae and immediately cranial to the tail coverts (Fig. 4A). It is marked by a slight eminence and a stout papilla bearing the downy uropygial circlets (Fig. 4A, B). The uropygial gland itself is well-developed, bilobed and heart-shaped. The cranialmost part of the gland is covered by the M. levator caudae (for comparison see Jakob and Ziswiler 1982; Zusi 1985). If and to what extent this muscle inserts at the uropygial gland could not be determined (Fig. 4C). The glands were on average 34.4 ± 2.7 mm wide, 32.2 ± 1.92 mm long, and 6.375 ± 0.634 mm thick, and weighed 3.46 ± 0.3 g. The relative gland mass (RGM) was 0.15 ± 0.025.

Morphology of the cormorant uropygial gland

The uropygial gland is a holocrine gland surrounded by a tough capsule consisting of connective tissue (e.g., Jakobs and Ziswiler 1982). This capsule continues as the interlobular septum separating the two lobes of the gland (Figs. 6A, 7A). The internal structure of the cormorant uropygial gland is demonstrated in the parasagittal (Fig. 5), the horizontal (Fig. 6), and the coronal plane (Fig. 7) in order to show the complex internal organization. From the external capsule originate internal septa that structure and support the glandular tubules that fill large parts of the gland (Figs. 5A, 6A, 7A). These tubules consist of a basal stratum germinativum, an intermediate layer, a secretory area and a degenerative layer (Lucas and Stettenheim 1972; Jakob and Ziswiler 1982). These layers can be clearly distinguished in the cormorant (Figs. 5E-G, 6D, E, 7F, G). Based on the relative thickness of the layers, the tubules can be divided in three zones (Lucas and Stettenheim 1972; Jakob and Ziswiler 1982). In the periphery (zone I), the stratum germinativum is well developed, the secretory area consists of several cell layers whereas the degenerative layer and the lumen are small if present at all (e.g., Figs. 5F, 6D). The middle zone (zone II) represents the largest part of the tubule with a thin stratum germinativum, the degenerative layers are thick, and tubules contain an increasingly large lumen filled with cell

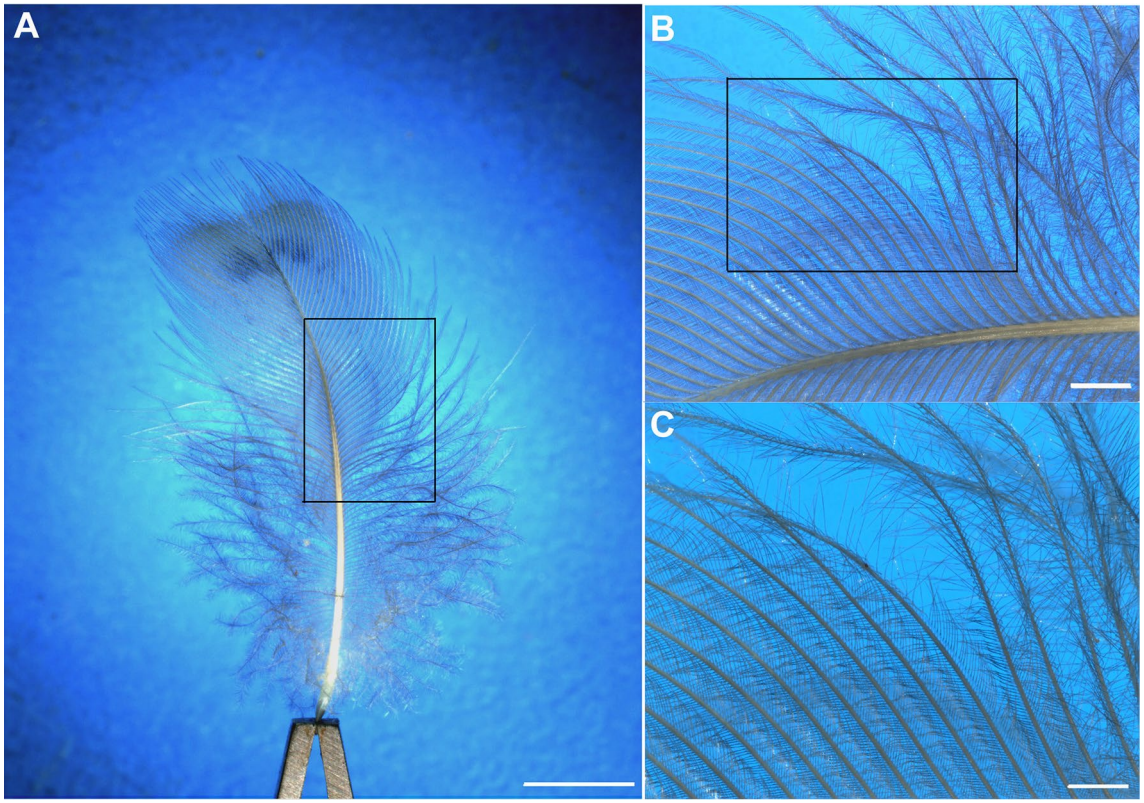

Fig. 3 Photograph of a feather from the ventral rump of an European Widgeon (*Mareca penelope*) demonstrating the morphology typical also for feathers from the breast and the back. **A**: overview, **B**, **C**: details of the transition zone of the closed and the open vane. Inset in **A** shows the location of the detail seen in **B**, inset in **B** shows location of detail depicted in **C**. Scale bars represent 5 mm (**A**), 1 mm (**B**), and 0.5 mm (**C**)

debris and secretion (Figs. 5E, F, G; 6E, 7G). In the innermost zone (zone III), the tubules have large inner lumina but only a very thin glandular epithelium. They converge to form collecting glandular ducts that ultimately lead to the papilla and the opening of the gland (Figs. 5A–E, 6A, C, 7A, D). Besides the collecting ducts, the papilla contains fat tissue, the feather follicles of the circlets as well as mechanoreceptive Pacini corpuscles, nerves and blood vessels (Figs. 5A, B, 6A, B, 7A-C).

Morphology of the pigeon uropygial gland

For comparison, we analyzed the uropygial gland of the rock pigeon. The rock pigeon does not have circlets. In stark contrast to the cormorant, the inner structure of the pigeon uropygial gland is less elaborate, with short glandular tubules that discharge in very large central storage reservoirs (Fig. 8A, B). The glandular epithelium is mostly confined to the inner wall of the capsule and the relatively few internal septa (Fig. 8C).

3D-reconstruction of the uropygial gland

In order to summarize the internal structure of the cormorant uropygial gland we, to our knowledge, for the first time three-dimensionally reconstructed the organ based on the parasagittal sections of the cormorant and pigeon (Fig. 9, see also supplementary movies 1–4). Based on confocal images and subsequent drawings of the internal segregation of the uropygial gland, 3D-models were constructed emphasizing the morphological differences between the two species. In cormorant, the gland is completely filled with glandular and secretion-filled tubules. The compact glandular tissue is subdivided by numerous secondary septa over the whole extent of the gland (supplementary movie 3). By contrast, in pigeon glandular tubules are restricted to the periphery close to the capsule, and the main part of the gland consists of a central lumen. Only few secondary septa are present (supplementary movie 4).

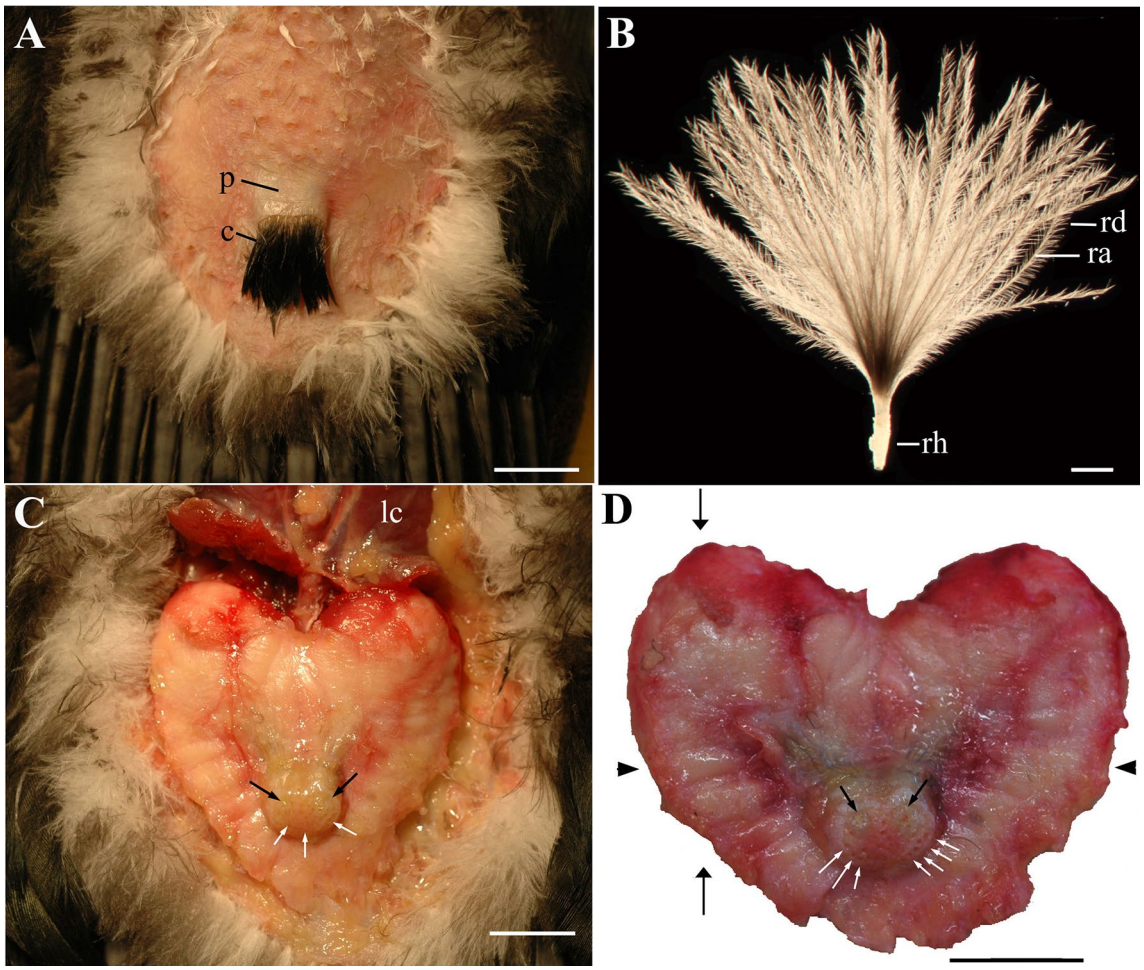

Fig. 4 Photographs of the dissection of the cormorant uropygial gland. **A** After removal of the feathers the gland is indicated by a slight prominence and the stout papilla bearing the circlets. **B** dark-field photograph of a circlet feather; **C**: After removal of the overlying skin the heart-shaped uropygial gland with the papilla appears. **D** ex situ photograph of the uropygial gland in dorsal view. Scale bars indicate 1 cm in **A**, **C**, **D**, and 1 mm in **B**. *c* circlet, *lc* m. levator caudae, *p* papilla, *ra* ramus, *rd* radius, *rh* rhachis. Black arrows indicate the location of the orifices, white arrows point to follicles of the circlet feathers. Large black arrows (Fig. 4D) on the left side of the gland indicate the parasagittal plane of section (see Fig. 5), the arrowheads indicate the coronal plane of section (see Fig. 7). The horizontal plane of section is parallel to the surface of the gland (compare Figs. 4D, 6)

Discussion

Cormorants are well known for their wing-spreading behavior, probably a necessity caused by their unusual feather structure. Cormorant cover feathers have a closed vane only next to the rhachis whereas the more distal parts of the barbs are not connected by barbules (this study, Grémillet et al. 2005; Srinivasan et al. 2014). This morphology causes a partial wettability. Functional advantages of this morphology are, e.g., reduced buoyancy, reduced energy costs during diving, and an increased foraging efficiency (Schmid et al. 1995; Grémillet et al. 2001; Ribak et al. 2005). However, only few water birds have such a feather structure. As we (this study) and others (Grémillet et al. 2005; Srinivasan et al. 2014) have shown by comparing diving ducks, i.e., the Tufted Duck, and dabbling ducks, i.e., the European Widgeon with the cormorant, this feather structure at first glance seems unrelated to ecology and foraging behavior. However, reduced buoyancy and reduced energy costs could be especially advantageous for a piscivorous hunter like the cormorant when compared to herbivorous ducks. The wing feathers of the cormorant are indistinguishable from the wing feathers of the tufted duck or the European Widgeon probably to ensure the functional integrity of the airfoils for flight. The effect of the wing-spreading behavior would then not be primarily a drying of the wings but exposure of a large part of the body to the sun and the wind to facilitate the evaporation of the water retained by the body plumage. Interestingly, it was hypothesized that despite the imperfect

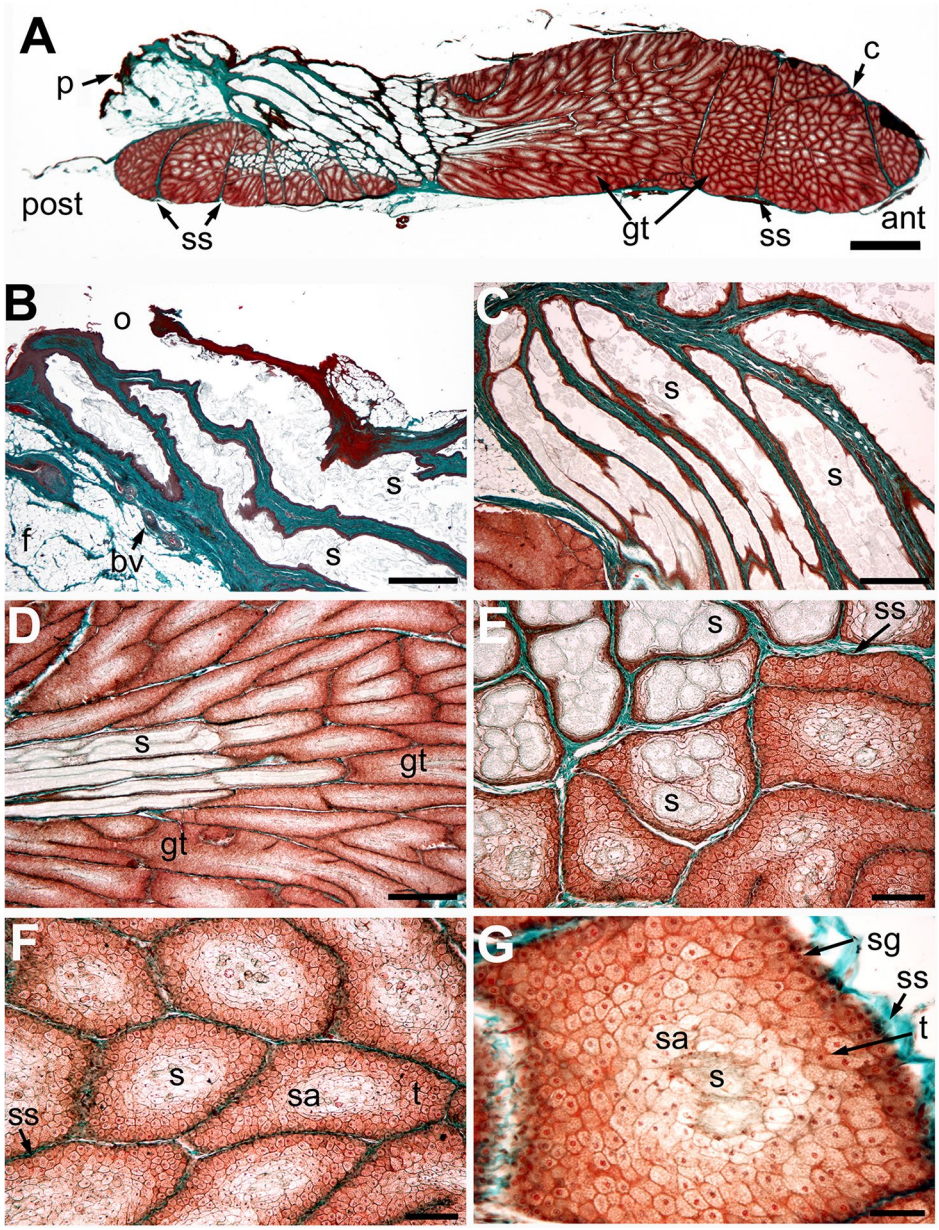

Fig. 5 Microphotographs of parasagittal sections through the uropygial gland of a cormorant arranged from the papilla to the peripheral glandular tubules. **A** overview of a parasagittal section demonstrating the gland filled with glandular tubules. Posterior is to the left. The section is located 2790 µm from the lateral-most edge of the gland. Scale bar: 2 mm. **B** Secretion-filled glandular ducts leading to the orifice of the papilla. The papilla is composed of fat and connective tissue (green) and contains blood vessels. The section is located 2700 µm from the lateral-most edge of the gland. Scale bar: 500 µm. **C** secretion-filled glandular ducts leading to the papilla. The section is located 2400 µm from the lateral-most edge of the gland. Scale bar: 500 µm. **D** glandular tubules converge to form light, secretion-filled glandular ducts of zone III (Lucas and Stettenheim 1972; Jakob and Ziswiler 1982). The glandular ducts can be distinguished by their larger lumen and the paucity of glandular tissue along their wall. The section is located 3200 µm from the lateral-most edge of the gland. Scale bar: 500 µm. **E** transition of glandular tubules to secretion-filled ducts in zone III. The section is located 4100 µm from the lateral-most edge of the gland. Scale bar: 100 µm. **F** glandular tubules separated by secondary septa, zone II. The section is located 3200 µm from the lateral-most edge of the gland. Scale bar: 100 µm. **G** Detail of a secretory tubule composed of the basal stratum germinativum, the transitory zone, and the secretory area of zone II. The section is located 1850 µm from the lateral-most edge of the gland. Scale bar: 50 µm. *ant* anterior, *bv* blood vessel, *c* capsule surrounding the gland, *f* fat tissue, *gt* glandular tubules, *o* orifice, *p* papilla, *s* secretion, *sa* secretory area, *sg* stratum germinativum, *ss* secondary septum, *t* transition zone

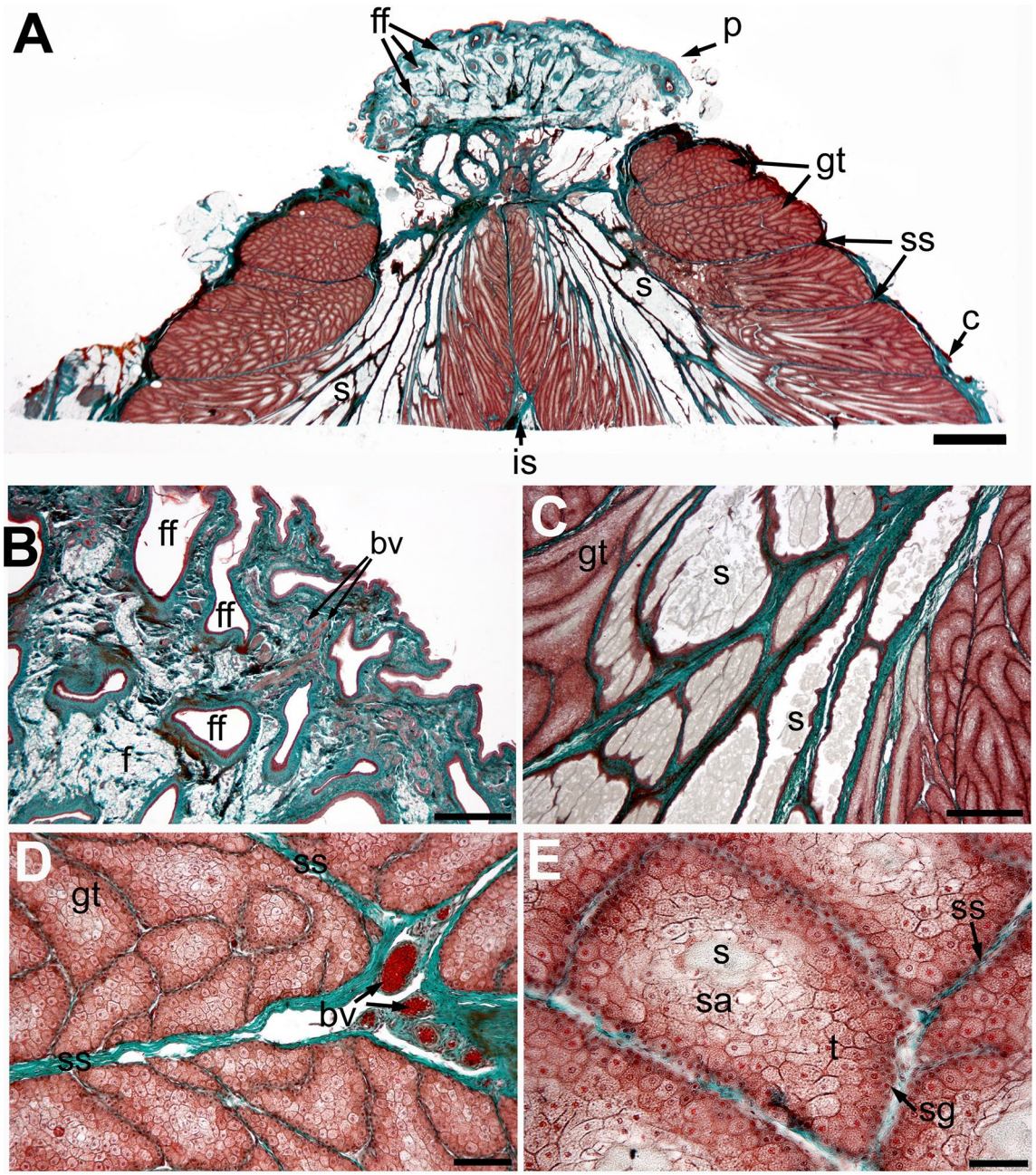

Fig. 6 Microphotographs of horizontal sections (parallel to the surface of the gland) through the posterior part of the uropygial gland of a cormorant. **A** Overview demonstrating the papilla containing the feather follicles of the circlets, the interlobular septum between the two lobes of the gland, and the glandular tubules converging in secretion-filled glandular ducts. The section is located 2600 µm below the dorsal edge of the papilla. Scale bar: 2 mm. **B** papilla with feather follicles, fat cells and blood vessels. The section is located 900 µm below the dorsal edge of the papilla. Scale bar: 500 µm. **C** glandular tubules and secretion filled ducts leading toward the papilla in zone III. The section is located 3030 µm below the dorsal edge of the papilla. Scale bar: 500 µm. **D** peripheral glandular tubules divided by secondary septa. The section is located 5030 µm below the dorsal edge of the papilla. Scale bar: 100 µm. **E** glandular tubule with stratum germinativum, transition zone, secretory area and secretion-filled lumen of zone II. The section is located 4800 µm below the dorsal edge of the papilla. Scale bar: 50 µm. *bv* blood vessel, *c* capsule surrounding the gland, *f* fat tissue, *ff* feather follicle, *gt* glandular tubules, *p* papilla, *s* secretion, *sa* secretory area, *sg* stratum germinativum, *ss* secondary septum, *t* transition zone

insulation accomplished by their feathers the wing-spreading behavior of cormorants may have facilitated the colonization of colder regions (Grémillet et al. 2001).

The morphology of the uropygial gland as well as the components of its secretion have been studied in an unparalleled study of 150 bird species by Jacob and Ziswiler

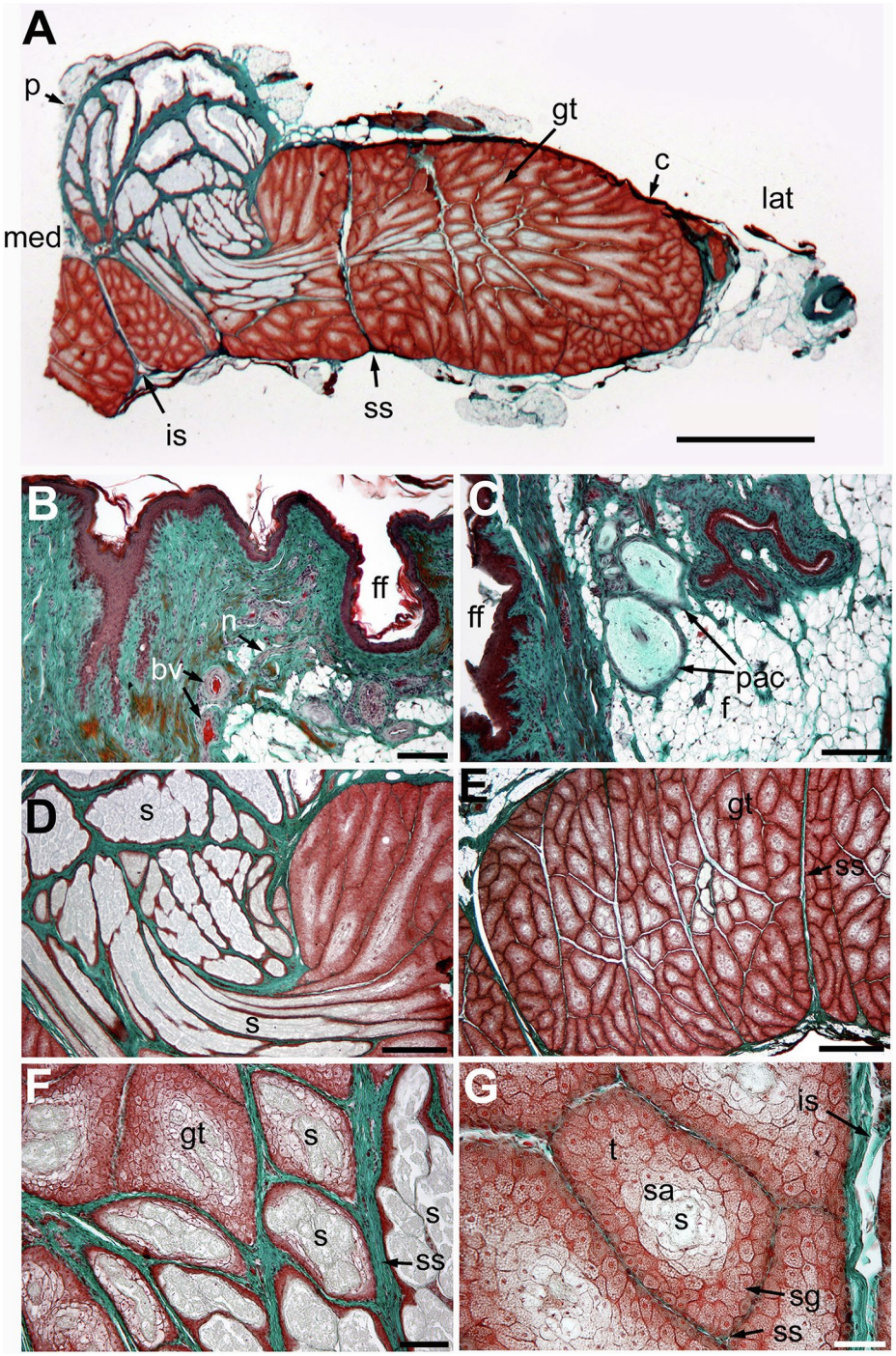

Fig. 7 Microphotographs of coronal sections through the left lobe of the uropygial gland of a cormorant. **A** overview showing the papilla, the secretion-filled glandular ducts, and the glandular tubules separated by secondary septa. Medial (med) is to the left, lateral (lat) to the right. The section is located 4980 µm anterior to the posterior edge of the gland. Scale bar: 2 mm. **B** papilla with feather follicle, blood vessels and nerves. The section is located 2180 µm anterior to the posterior edge of the gland/papilla. Scale bar: 100 µm. **C** papilla with feather follicle, fat tissue, and Vater Pacini corpuscles. The section is located 4800 µm anterior to the posterior edge of the gland. Scale bar: 100 µm. **D** secretion-filled glandular ducts of zone III close to the papilla. The section is located 4980 µm anterior to the posterior edge of the gland. Scale bar: 500 µm. **E** glandular ducts separated by secondary septa. The section is located 2980 µm anterior to the posterior edge of the gland. Scale bar: 500 µm. **F** glandular tubules in the transition of zone II and III. The section is located 7080 µm anterior to the posterior edge of the gland. Scale bar: 100 µm. **G** Detail of a secretory tubule of zone II composed of the basal stratum germinativum, the transitory zone, and the secretory area. The section is located 9480 µm anterior to the posterior edge of the gland. Scale bar: 50 µm. *bv* blood vessel, *c* capsule surrounding the gland, *f* fat tissue, *ff* feather follicle, *gt* glandular tubules, *is* interlobular septum, *n* nerve, *p* papilla, *pac* Vater pacini corpuscle, *s* secretion, *sa* secretory area, *sg* stratum germinativum, *ss* secondary septum, *t* transition zone

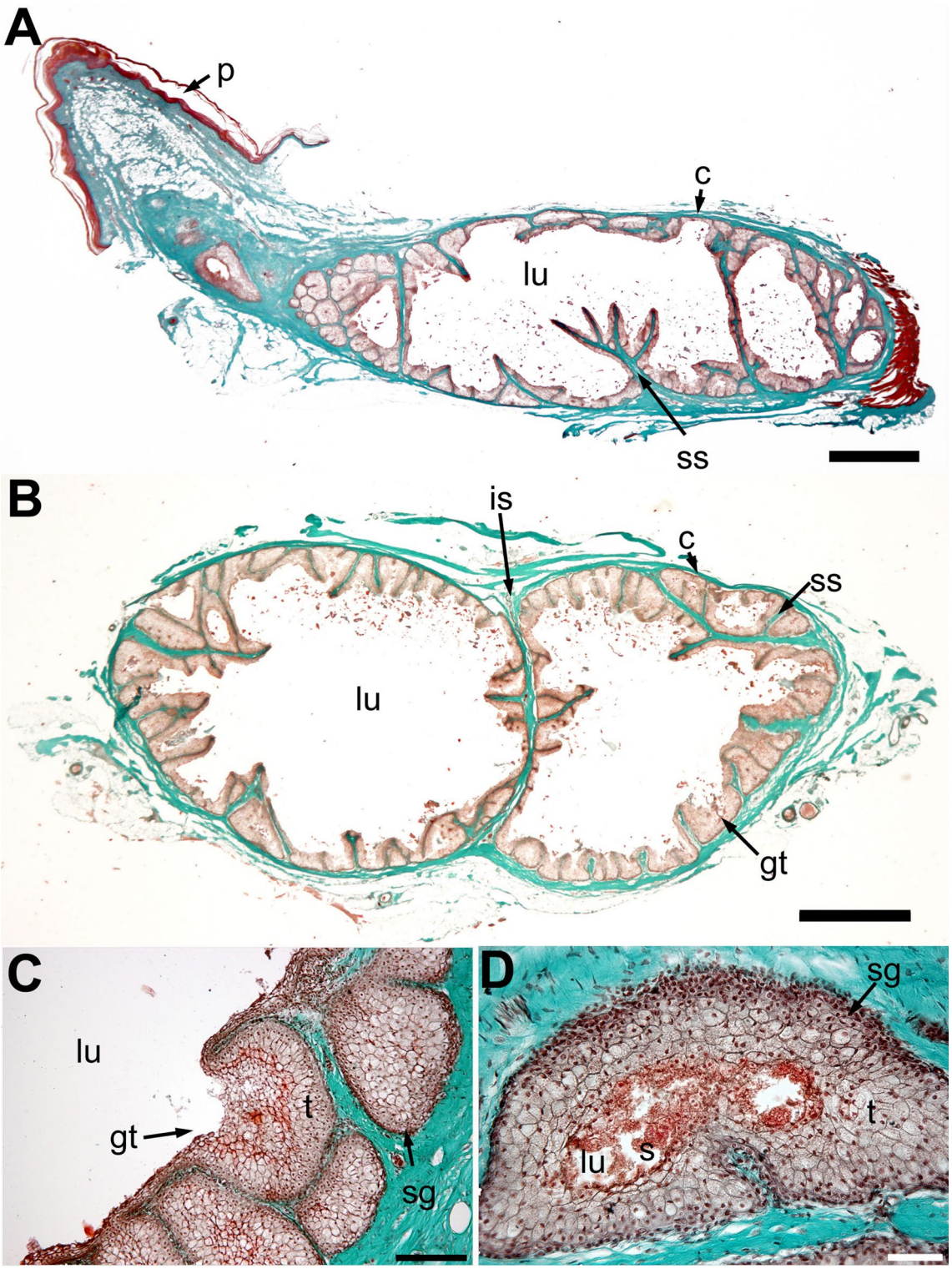

Fig. 8 Microphotographs of sections through the uropygial gland of the rock pigeon. **A** parasagittal section, posterior is to the left. The section is located 900 µm from the lateral edge of the gland. Scale bar 1000 µm. **B** coronal section. The section is located 3000 µm posterior to the anterior edge of the gland. Scale bar 1000 µm. **C** coronal section through a glandular tubule opening into the lumen. The section is located 3900 µm posterior to the anterior edge of the gland. Scale bar 100 µm. **D** coronal section through a glandular tubule, zone II. The section is located 9480 µm posterior to the anterior edge of the gland. Scale bar 50 µm. *c* capsule surrounding the gland, *gt* glandular tubules, *is* interlobular septum, *lu* lumen with cell debris and secretion, *p* papilla, *s* secretion, *sg* stratum germinativum, *ss* secondary septum, *t* transition zone

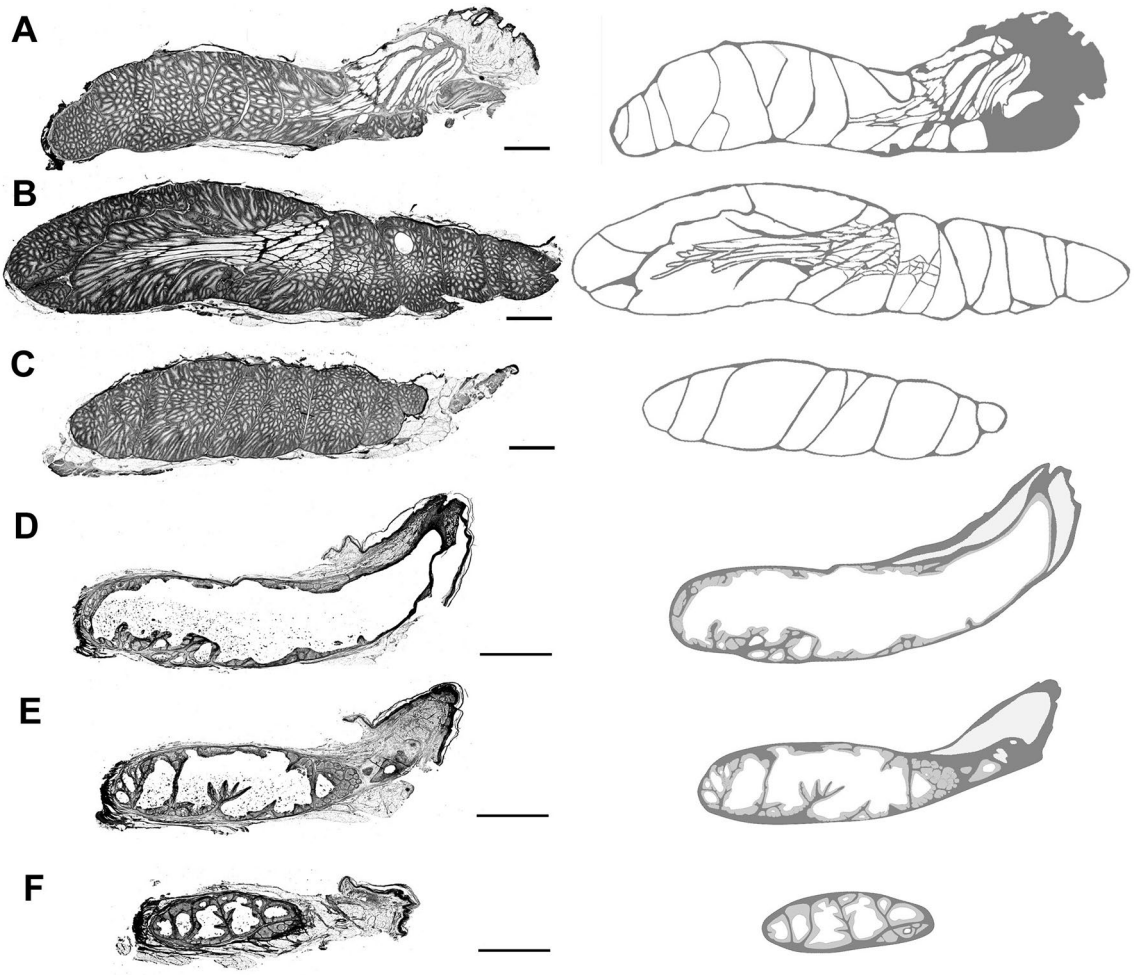

Fig. 9 Left row: Confocal micrographs of sagittal sections through the uropygial gland of a cormorant (**A**–**C**) and a pigeon (**D**–**F**). Right row: corresponding drawings serving as basis for the 3D-reconstructions. In cormorant, the whole gland is filled with glandular and secretion-filled tubules. In pigeon, grey areas indicate glandular tubules, light grey areas in the region of the papilla indicate fat cells incorporated in connective tissue. **A**, **D**: sections through the papilla, **B**, **E**: sections through the intermediate portion of the gland, **C**, **F**: sections through the lateral portion of the gland. Scale bars: 2 mm

(1982). Almost all birds have bilobular uropygial glands and birds associated with water usually have larger glands than purely terrestrial birds but beyond this no further generalizations were possible due to the large variability (Jakob and Ziswiler 1982, but see Montalti and Salibián 2000; Chiale et al. 2014). There was no significant difference between diving and dabbling ducks. The relative size of the uropygial gland in our cormorant sample was somewhat smaller, the length of the gland somewhat larger than the values given by Jacob and Ziswiler (1982). As no standard deviations were presented by the authors it is hard to estimate the relevance of this discrepancy.

More recently, the uropygial glands of a number of species some of which had already been examined by Jakob and Ziswiler (1982) have been described in some detail, e.g., moorhen (Sawad 2006), white stork (Kozlu et al. 2011), goose (Shafiian and Mobini 2014), duck (Hassanin et al. 2021), hooded grebe (Chiale et al. 2022), caracara (Chiale et al. 2016, 2017), kiwi (Reynolds et al. 2017), eared dove (Chiale et al. 2019), rock pigeon (Hassanin et al. 2021; this study), and monk parakeet (Carril et al. 2020). The general histological structure of the gland is similar in all birds investigated so far, including the Great Cormorant examined in the present study. As established by Lucas and Stettenheim (1972) and Jakob and Ziswiler (1982), the glandular tubules can be divided into three zones: the peripheral zone I, a middle zone II, and the innermost zone III. These zones differ in the thickness and shape of their subdivisions, i.e., the stratum germinativum, the intermediate, the degenerative, and the secretory layers. The main histological differences between species seem to be related to the presence or absence of central storage chambers which are mostly present in purely terrestrial birds as eared doves (Chiale et al. 2019), rock pigeon (this study, Hassanin et al. 2021),

caracaras (Chiale et al. 2016, 2017), kiwi (Reynolds et al. 2017), and monk parakeet (Carril et al. 2020) but absent in most aquatic birds as the hooded grebe (Chiale et al. 2022), duck (Hassanin et al. 2021), penguins (Chiale et al. 2014) and cormorant (this study). Thus, aquatic birds continuously in need of uropygial secretions for feather maintenance seem to release the secretions constantly whereas terrestrial birds secrete only periodically and therefore have to store the secretions until need. However, this putative relationship of the presence of a primary storage chamber with the lifestyle of the bird does not generally hold true: the aquatic moorhen and sea gulls have a large primary storage chamber (Sawad 2006; Abd Al-Khazraji 2017), the coastal scuas have no primary storage chamber (Chiale et al. 2014;). In conclusion, the structure of the uropygial gland seems to be only weakly correlated with phylogeny or lifestyle (Jakob and Ziswiler 1982; Montalti and Salibián 2000; Chiale et al. 2014). The cormorant's grooming behavior, i.e., spreading the uropygial secretion onto the feathers by head rubbing and preening seems to be indistinguishable from other birds (Johnsgard 1993) but is particularly intense during the drying period (Ross 1976). As the cormorant's uropygial gland structure resembles that of many other aquatic birds, it remains to be seen how the composition of the cormorant uropygial secretion differs from other birds.

Therefore, we analyzed the biochemical components of the cormorant's uropygial secretion and compared them with the secretion of the Muscovy Duck (see accompanying paper, Holste et al. submitted). There was a stark difference between the two species: the cormorant's secretion is made up of more than 1,000 compounds consisting of methyl-branched aliphatic carboxylic esters with very variable chain lengths. No dicarboxylic acids and other fatty acid derivatives were found in the cormorant. By contrast, the Muscovy Duck's secretion is dominated by the two esters octadecyl and eicosyl 2,4,6-trimethyloctanoate. It also contains dicarboxylic acids. Water contact angle measurements of the secretions showed that the secretion of the Muscovy Duck has higher water repellence than that of the cormorant. Nevertheless, contact angle measurements of untreated and degreased feathers yielded no significant differences between the two conditions. This indicates that the physical construction of the feather surface plays an important, possibly the major role for their hydrophobicity thus supporting former studies (e.g., Rijke 1968; Grémillet et al. 2005; Srinivasan et al. 2014).

Supplementary Information The online version contains supplementary material available at https://doi.org/10.1007/s10336-022-02042-8.

Acknowledgements We wish to thank M. Betz and U. Ledebur for supplying the feather samples of the Tufted Duck and the widgeon, M. Roller, L. Reese and J. Golbach for supplying feather samples of Muscovy Ducks, F. Lohmar for supplying the cormorant carcasses, H. Lübbert for lab space, F. Paris for advice concerning histology, and T. Stützel for support with photography. The experiments comply with the current animal protection act of Germany.

Author contributions NS: dissection, histology, data analysis; SS: 3D-reconstruction, AM: code, 3D-reconstruction, writing and editing of manuscript, CD: study design, data analysis, writing and editing of manuscript.

Funding Open Access funding enabled and organized by Projekt DEAL. Not applicable.

Data availability The material is being held at the Dept. General Zoology & Neurobiology, Ruhr-University Bochum,

Code availability Image processing scripts are available on request from Axel Mosig.

Declarations

Conflict of interest Not applicable.

References

Abd Al-Khazraji KI (2017) Histological and morphological study of the uropygial gland in gull (*Larus canus*). Diyala J pure Sci 13:230–239. https://doi.org/10.24237/djps.1303.308A

Amo L, Avilés JM, Parejo D, Pena A, Rodrìguez J, Tomás G (2012) Sex recognition by odour and variation in the uropygial gland secretion in starlings. J Anim Ecol 81:605–613. https://doi.org/10.1111/j.1365-2656.2011.01940.x

Bandyopadhyay A, Bhattacharyya S (1999) Influence of fowl uropygial gland and its secretory lipid components on the growth of skin surface fungi of fowl. Indian J Exp Biol 37:1218–1222. https://pubmed.ncbi.nlm.nih.gov/10865889/

Carril J, Chiale MC, Barbeito CG (2020) The uropygial gland of the monk parakeet *Myiopsitta monachus*: Histology, morphogenesis, and evolution within Psittaciformes (Aves). Evol Dev 22:269–282. https://doi.org/10.1111/ede.12327

Caspers BA, Marfull R, Dannenhaus T, Komdeur J, Korsten P (2022) Chemical analysis reveals sex differences in the preen gland secretion of breeding Blue Tits. J Ornithology 163:191–198. https://doi.org/10.1007/s10336-021-01921-w

Chiale MC, Fernández PE, Gimeno EJ, Barbeito C, Montalti D (2014) Morphology and histology of the uropygial gland in Antarctic birds: relationship with their contact with the aquatic environment? Austral J Zool 62:157–165. https://doi.org/10.1071/ZO13103

Chiale MC, Montalti D, Flamini MA, Fernández P, Gimeno E, Barbeito CG (2016) Histological and histochemical study of the uropygial gland of chimango caracara *(Milvago chimango vieillot*, 1816).

Biotech Histochem 91:30–37. https://doi.org/10.3109/10520295.2015.1068953
Chiale M, Montalti D, Flamini MA, Barbeito CG (2017) The uropygial gland of the southern caracara (*Caracara plancus*; Falconidae: Falconinae): histological and histochemical aspects. Acta Zoologica 98:245–251. https://doi.org/10.1111/azo.12171
Chiale MC, Carrill J, Montalti D, Barbeito CG (2022) Comparative morphology and histochemistry of the uropygial gland of the endangered and endemic Hooded Grebe (*Podiceps gallardoi*, Podicipediformes). Acta Zoologica 103:90–98. https://doi.org/10.1111/azo.12357
Chiale MC, Carril1 C, Montalti D, Barbeito CG (2019) The uropygial gland of the Eared Dove and its evolutionary history within the Columbiformes (Aves). J Ornithol 160:1171–1181. https://doi.org/10.1007/s10336-019-01691-6
Elder WH (1954) The oil gland of birds. Wilson Bull 66:6–31
Giraudeau M, Duval C, Guillon N, Bretagnolle V, Gutierrez C, Heeb P (2010) Effects of access to preen gland secretions on mallard plumage. Naturwissenschaften, 577–581. https://doi.org/10.1007/s00114-010-0673-z
Goldner J (1938) A modification of the Masson trichrome technique for routine laboratory purposes. Am J Pathol 14:237–243
Gomori G (1950) Aldehyde-fuchsin: a new stain for elastic tissues. Am J Clin Pathol 20:665–666
Grémillet D, Wanless S, Carss DN, Linton D, Harris MP, Speakman JR, Le Maho Y (2001) Foraging energetics of arctic cormorants and the evolution of diving birds. Ecology Lett 4:180–184. https://doi.org/10.1046/j.1461-0248.2001.00214.x
Grémillet D, Chauvin C, Wilson R, Le Maho Y, Wanless S (2005) Unusual feather structure allows partial plumage wettability in diving great cormorants *Phalacrocorax carbo*. J Avian Biol 36:57–63. https://doi.org/10.1111/j.0908-8857.2005.03331.x
Hassanin A, Shoeib M, Massoud D (2021) Micro- and macroanatomical features of the uropygial gland of duck (*Anas platyrhynchos*) and pigeon (*Columba livia*). Biotech & Histochem 96:213–222. https://doi.org/10.1080/10520295.2020.1782990
Jacob J, Balthazart J, Schoffeniels E (1979) Sex differences in the chemical composition of uropygial gland waxes in domestic ducks. Biochem Syst Ecol 7:149–153. https://doi.org/10.1016/0305-1978(79)90024-3
Jacob J, Ziswiler V (1982) The uropygial gland. In: Farner D, King J, Parkes K (eds) Avian Biology IV. Academic Press, New York, pp 199–324
Johnsgard P (1993) Cormorants, darters and pelicans of the world. Smithsonian Institution Press, London, Washington, pp 226–234
Johnston D (1988) A morphological atlas of the avian uropygial gland. Bull British Museum (Natural History). Zoology Series 54(5):199–259
Kozlu T, Akaydin Bozkurt Y, Ates S (2011) A macroanatomical and histological study of the uropygial gland in the White Stork (*Ciconia cicionia*). Int J Morphol 39(3):723–726. https://doi.org/10.4067/S0717-95022011000300010
Lucas A, Stettenheim P (1972) Avian anatomy: integument. U.S. Department of Agriculture, Washington, D.C.
Møller AP, Erritzøe J, Rózsa L (2010) Ectoparasites, uropygial glands and hatching success in birds. Oecologia 163:303–311. https://doi.org/10.1007/s00442-009-1548-x
Montalti D, Salibián A (2000) Uropygial gland size and avian habitat. Ornitologia Neotropical 11:297–306
Moreno-Rueda G (2017) Preen oil and bird fitness: a critical review of the evidence. Biol Rev 92:2131–2143. https://doi.org/10.1111/brv.12324
Peng H, Ruan Z, Long F, Simpson JH, Myers EW (2010) V3D enables real-time 3D visualization and quantitative analysis of large-scale biological image data sets. Nature Biotech 28:348–353. https://doi.org/10.1038/nbt.1612
Quintana F, Wilson R, Yorio P (2007) Dive depth and plumage air in wettable birds: the extraordinary case of the imperial cormorant. Mar Ecol Prog Ser 344:299–310. https://doi.org/10.3354/meps334299
Reneerkens J, Piersma T, Sinninghe Damsté JS (2005) Switch to diester preen waxes may reduce avian nest predation by mammalian predators using olfactory cues. J Exp Biol 208:4199–4202. https://doi.org/10.1242/jeb.01872
Reynolds SM, Castro I, Alley MR, Cunningham SJ (2017) *Apteryx spp*. (Kiwi) possess an uropygial gland: anatomy and pathology. Eur J Anat 21(2):125–139
Ribak G, Weihs D, Arad Z (2005) Water retention in the plumage of diving great cormorants *Phalacrocorax carbo sinensis*. J Avian Biol 36(89/95):2005
Rijke A (1968) The water repellency and feather structure of cormorants, Phalacrocoracidae. J Exp Biol 48:185–189. https://doi.org/10.1242/jeb.48.1.185
Rijke A, Jesser W (2011) The water penetration and repellency of feathers revisited. The Condor 113(2):245–254
Ross RK (1976) Notes on the behaviour of captive Great Cormorants. Wilson Bulletin 88:143–145
Sawad AA (2006) Morphological and histological study of uropygial gland in moorhen (*G. gallinula chloropus chloropus*). Int J Poultry Sci 5(10):938–941
Schindelin J, Arganda-Carreras I, Frise E, Kaynig V, Longair M, Pietzsch T, Preibisch S, Rueden C, Saalfeld S, Schmid B, Tinevez J-Y, White DJ, Hartenstein V, Eliceiri K, Tomancak P, Cardona A (2012) Fiji: an open-source platform for biological-image analysis. Nat Methods 9:676–682. https://doi.org/10.1038/nmeth.2019
Schmid D, Grémillet D, Culik B (1995) Energetics of underwater swimming in the great cormorant (*Phalacrocorax carbo sinensis*). Mar Biol 123:875–881. https://doi.org/10.1007/BF00349133
Sellers R (1995) Wing-spreading behaviour of the cormorant. Ardea 83:27–36
Shafiian A H, Mobini B (2014) Histological and histochemical study on the uropygial gland of the goose (*Anser anser*). Bulg J Vet Med 17:1–8. http://tru.uni-sz.bg/bjvm/bjvm.htm
Shawkey M, Pillai S, Hill G (2003) Chemical warfare? Effects of uropygial oil on feather-degrading bacteria. J Avian Biol, 345–349. https://doi.org/10.1111/j.0908-8857.2003.03193.x
Soini HA, Schrock SE, Bruce KE, Wiesler D, Ketterson ED, Novotny MV (2007) Seasonal variation in volatile compound profiles of preen gland scretions of the dark-eyed Junco (*Junco hyemalis*). J Chem Ecol 33:183–198. https://doi.org/10.1007/s10886-006-9210-0
Soler JJ, Martín-Vivaldi M, Peralta-Sánchez JM, Arco L, Juárez-García-Pelayo N (2014) Hoopoes color their eggs with antimicrobial uropygial secretions. Naturwissenschaften 101:697–705. https://doi.org/10.1007/s00114-014-1201-3
Srinivasan S, Chhatre S, Guardado J, Park K-C, Parker A, Rubner M, McKinley G, Cohen R (2014) Quantification of feather structure, wettability and resistance to liquid penetration. J R Soc Interface 11:1–11. https://doi.org/10.1098/rsif.2014.0287
Whittaker DJ, Rosvall KA, Slowinski SP, Soini HA, Novotny MV, Ketterson ED (2018) Songbird chemical signals reflect uropygial gland androgen sensitivity and predict aggression: implications for the role of the periphery in chemosignaling. J Comp Physiol A 204:5–15. https://doi.org/10.1007/s00359-017-1221-5
Zusi RL (1985) Muscles of the neck, trunk and tail of the noisy scrubbird, *Atrichornis clamosus*, and superb lyrebird, *Menura novaehollandiae* (Passeriformes: Atrichornithidae and Menuridae). Rec Austral Museum 37:229–242